

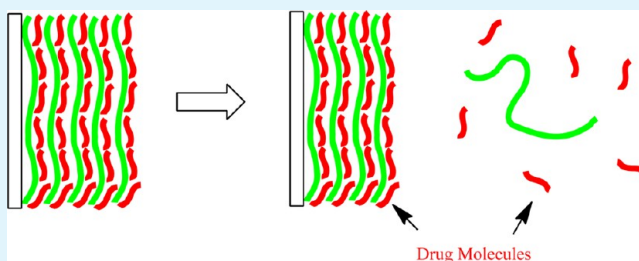
# Release of Polyphenolic Drugs from Dynamically Bonded Layer-by-Layer Films

Lin Zhou, Mao Chen, Lili Tian, Ying Guan, and Yongjun Zhang\*

State Key Laboratory of Medicinal Chemical Biology and Key Laboratory of Functional Polymer Materials, Institute of Polymer Chemistry, College of Chemistry, Nankai University, Tianjin 300071, China

## Supporting Information

**ABSTRACT:** Layer-by-layer (LbL) assembled films have been exploited for surface-mediated drug delivery. The drugs loaded in the films were usually released via diffusion or the degradation of one of the film components. Here we demonstrate that drug release can also be achieved by exploiting the dynamic nature of hydrogen-bonded LbL films. The films were fabricated from tannic acid (TA), a model polyphenolic drug, and poly(vinyl pyrrolidone) (PVPON). The driving force for the film buildup is the hydrogen bonding between the two components, which was confirmed by Fourier transform infrared (FTIR) spectra. The film growth is linear, and the growth rate of the film decreases with increasing assembly temperature. Because of the reversible/dynamic nature of hydrogen bonding, when soaked in aqueous solutions, the PVPON/TA films disassemble gradually and thus release TA to the media. The release rate of TA increases with increasing pH and temperature but decreases with increasing ionic strength. Scanning electron microscopy (SEM) studies on the surface morphology of the film during TA release reveal that the film surface becomes smoother and then rougher again because of the dewetting of the film. The released TA can scavenge ABTS<sup>•+</sup> cation radicals, indicating it retains its antioxidant activity, a major biological activity of polyphenols.



**KEYWORDS:** dynamic bonds, hydrogen bonds, layer-by-layer assembly, drug release, polyphenolic drug, antioxidant activity

## INTRODUCTION

Layer-by-layer (LbL) assembly has been widely used to fabricate thin films from polymer pairs with complementary functional groups because of its advantages over other methods, such as no limit to the size and shape of the substrates, easy control over the film thickness and composition, and so on.<sup>1–3</sup> One important application of LbL films is for drug delivery.<sup>4–6</sup> For this purpose, two general strategies have been developed. In the first strategy, drugs are encapsulated in LbL microcapsules, and the LbL films act as diffusion barriers.<sup>7–9</sup> As the permeability of the capsule wall can be tuned by pH, ionic strength,<sup>10</sup> temperature,<sup>11</sup> and bilayer number of the coatings,<sup>12</sup> controlled drug release can be achieved by changing these factors. In the second strategy, drugs are integrated into the macroscopic planar LbL films. They are released via diffusion<sup>13,14</sup> or the degradation of one of the film components.<sup>15–17</sup> For example, LbL films have been fabricated from siRNA (drug) and degradable poly( $\beta$ -amino ester)s. siRNA was released upon the degradation of poly( $\beta$ -amino ester).<sup>15</sup> In these surface-mediated drug delivery systems, the LbL films may act as not only a reservoir for the active therapeutic cargo but also a coating to modulate surface properties.<sup>6</sup>

Here we demonstrate a new drug release strategy, i.e., releasing drug from LbL films via the gradual disassembly of the films, which are linked with dynamic bonds. Dynamic bonds are

chemical bonds which can selectively undergo reversible breaking and reformation, usually under equilibrium conditions.<sup>18</sup> Noncovalent dynamic bonds include supramolecular interactions, such as  $\pi$ - $\pi$  stacking, hydrogen bonding, and so on, while dynamic covalent bonds are covalent bonds that can break and reform under appropriate conditions without irreversible side reactions.<sup>18</sup> Because of the reversible/dynamic nature of these bonds, polymers containing these bonds present dynamic properties such as a changeable and tunable constitution even after polymerization; therefore, they were named as “dynamers” or dynamic polymers.<sup>18–20</sup> Many dynamic bonds, such as hydrogen bonding<sup>21–26</sup> and charge transfer interaction,<sup>27,28</sup> have been used as driving forces for the fabrication of LbL films.<sup>29</sup> Because of the reversible/dynamic nature of these bonds, LbL films linked with dynamic bonds, or dynamic LbL films, will also have a changeable and tunable constitution, just like dynamic polymers. Particularly, these films can undergo a gradual disassembly under proper conditions,<sup>30–33</sup> and therefore may be used for sustained drug release.

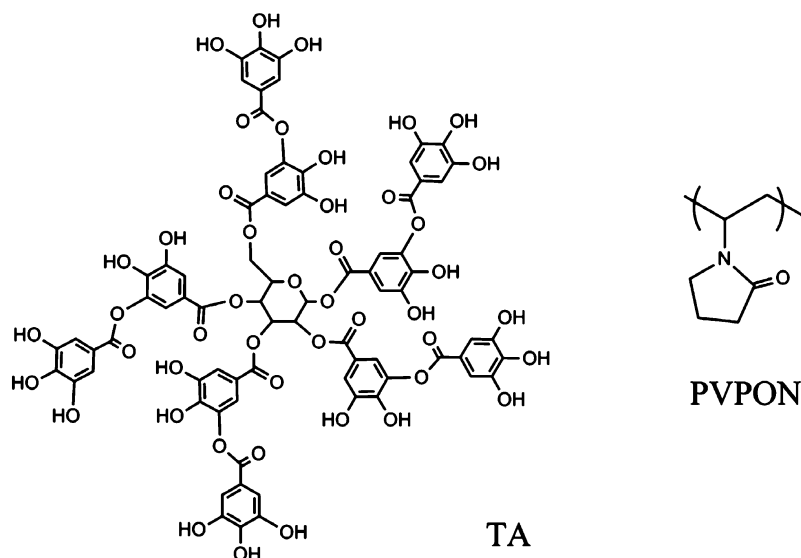
Hydrogen-bonded LbL films are typical dynamic LbL films. Previously it was reported that some hydrogen-bonded LbL

**Received:** September 2, 2012

**Accepted:** April 2, 2013

**Published:** April 2, 2013

Scheme 1. Chemical Structures of TA and PVPON



films or capsules gradually disintegrate when immersed in water.<sup>30–32</sup> Here we demonstrate that this property can be exploited to achieve the sustained release of polyphenolic drugs. It was reported that plant polyphenols possess various biological activities, such as antitumor, antimicrobial, enzyme inhibitory, and pro- or antimutagenic properties.<sup>34,35</sup> The inhibition of tumorigenesis by tea polyphenols has been demonstrated in different animal models for various cancers.<sup>36</sup> Many plant polyphenols, including epigallocatechin gallate, curcumin, luteolin, and resveratrol, are under intensive investigation as possible anticancer agents.<sup>37</sup> On the other side, delivery systems for polyphenols are also under investigation as they are expected to solve the problems such as low bioavailability and short half-life.<sup>37,38</sup> Here tannic acid (TA), a natural hydrolyzable tannin (Scheme 1), was used as a model polyphenolic drug. Like other plant polyphenols, the biological activity of TA as an antimutagenic, anticarcinogenic, antimicrobial, antioxidant, and antibacterial agent has already been revealed.<sup>39</sup> Here hydrogen-bonded LbL films were fabricated from TA and poly(vinyl pyrrolidone) (PVPON). We showed that because of the reversibility of hydrogen bonding the films gradually disassemble and thus release TA into the media. It is noteworthy that TA-containing LbL films,<sup>40</sup> including hydrogen bonded ones,<sup>41–43</sup> have been reported by several groups. Particularly Erel-Unal and Sukhishvili<sup>41</sup> studied the instability of TA/PVPON films in high pH solutions, where the films were quickly destroyed by the direct breakage of the hydrogen bonds as a result of the dissociation of the phenolic hydroxyl groups. In contrast, here we studied the gradual disassembly of the films under conditions of equilibrium control and further used it for the sustained release of TA.

## EXPERIMENTAL SECTION

**Materials.** Poly(vinyl pyrrolidone) (PVPON,  $M_w = 10\,000$ ), tannic acid (TA), and 2,2-azino-bis(3-ethylbenzothiazoline-6-sulfonic acid) diammonium salt (ABTS) were purchased from Sigma-Aldrich. The chemicals were used as received without further purification. NKA-9 macroporous adsorption resin was purchased from Tianjin Nankai Hecheng S&T Co. Ltd. It was pretreated according to the user's manual before use.

**Film Fabrication.** Quartz slides with a size of  $44\text{ mm} \times 10\text{ mm} \times 1\text{ mm}$  were used as substrate for the film fabrication. For Fourier transform infrared (FTIR) and scanning electron microscopy (SEM) studies, silicon wafers were used as substrate. Before use the substrates were cleaned in boiling piranha solution (3:7 v/v  $\text{H}_2\text{O}_2\text{--H}_2\text{SO}_4$  mixture) (*caution: this solution is extremely corrosive!*), rinsed with deionized (DI) water thoroughly, and then dried. The pH of the PVPON and TA solutions (0.5 mg/mL) was adjusted to 3.0 using 0.1 M HCl. To fabricate the LbL films, the substrates were immersed in PVPON and TA alternately, each for 5 min, intermediated with 1 min washing in  $10^{-3}$  M HCl. This cycle was repeated until the desired bilayer number was reached. The resultant film is denoted as “(PVPON/TA)<sub>n</sub>”, which means the film is fabricated from PVPON and TA with a bilayer number of *n*.

**TA Release.** To measure the release kinetics of TA, the PVPON/TA films (60 bilayer, unless otherwise specified) were immersed in 6 mL of release media (usually 20 mM pH 7.5 phosphate buffer, unless otherwise specified). Temperature was controlled with a refrigerated circulator. At appropriate intervals, the release media were removed, and the same volume of fresh media with the same temperature was added. Concentration of TA in the release media was determined using UV/vis spectroscopy at a wavelength of 278 nm.

**Antioxidant Activity of the Released TA.** Cation radicals of ABTS ( $\text{ABTS}^{+\bullet}$ ) was prepared according to refs 44 and 45. Briefly, 89  $\mu\text{L}$  of 0.14 M  $\text{K}_2\text{S}_2\text{O}_8$  was added to 5 mL of  $7 \times 10^{-3}$  M ABTS aqueous solution under stirring. The mixture was left overnight in dark at room temperature and then stored in dark. Macroporous adsorption resin (NKA-9) was treated with diluted  $\text{ABTS}^{+\bullet}$  solution for a period of 12 h. It was then washed with DI water thoroughly. The resulting  $\text{ABTS}^{+\bullet}$ -loaded resin was blue in color.

The  $\text{ABTS}^{+\bullet}$ -loaded resin was then soaked in pH 8.5 phosphate buffer. A (PVPON/TA)<sub>150</sub> film was dipped into the medium. The decoloration of the resin with time was recorded with a digital camera. The color change of the resin in the absence of PVPON/TA film was recorded simultaneously.

**Other Characterizations.** UV–vis absorption spectra were measured on a TU 1810PC UV–vis spectrophotometer (Purkinje General, China). Fourier transform infrared (FTIR) spectra were measured on a Bio-Rad FTS-6000 spectrometer operating at  $8\text{ cm}^{-1}$  resolution. SEM images were recorded on an FEI NanoSEM 430 Scanning Electron Microscope. Atomic force microscopy (AFM) images were acquired using a Benyuan CSPM5000s scanning probe microscope in tapping mode.

## RESULTS AND DISCUSSION

**Fabrication of PVPON/TA Films.** The LbL films were fabricated from PVPON and TA, whose structures were shown in Scheme 1. Using quartz slides as substrates, the film growth was facily monitored by UV–vis absorption spectrometry. As shown in Figure 1, the film presents two absorption bands at

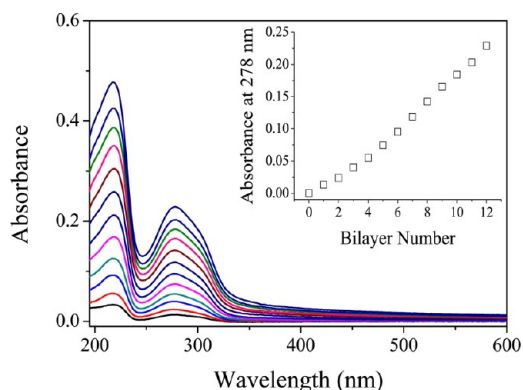


**Figure 1.** UV–vis absorption spectra of PVPON/TA films with various bilayer numbers (1–12). Inset: Plot of absorbance at 278 nm against bilayer number.

218 and 278 nm, respectively. Both bands can be assigned to the absorption of phenyl groups in TA, indicating the successful incorporation of TA in the film. The film grows almost linearly, as indicated by the almost linear relationship between the film absorbance and bilayer numbers as shown in the inset of Figure 1. Previously Erel-Unal and Sukhishvili<sup>41</sup> studied the assembly of PVPON and TA using ellipsometry technique and found a similar linear growth.

The driving force for the film buildup is expected to be the hydrogen bonding between the two components. The hydrogen donor and acceptor are TA and PVPON, respectively. To confirm this, the interaction between PVPON and TA in the self-assembled films was studied by IR spectroscopy. For this purpose, a 100-bilayer film was fabricated on a silicon wafer, and its FTIR spectra were measured. For comparison, FTIR spectra of pure PVPON and TA were also measured. As shown in Figure 2A, the absorption band at 1674  $\text{cm}^{-1}$  in the IR spectra of PVPON is assigned to the stretching vibration of carbonyl groups. This band shifts to 1655  $\text{cm}^{-1}$  in the spectra of the LbL film, suggesting the formation of intermolecular hydrogen bonds between the carbonyl groups in PVPON and the hydroxyl groups in TA. Meanwhile the stretching band of the carbonyl groups in TA shifts from 1717 to 1732  $\text{cm}^{-1}$ . The result suggests the carbonyl groups in TA are originally bonded with hydroxyl groups via intramolecular hydrogen bonds. These bonds partially break as a result of the formation of intermolecular hydrogen bonds between PVPON and TA in the film. The O–H stretching band of the hydroxyl groups in TA also shifts from 3400 to 3280  $\text{cm}^{-1}$  (Figure 2B), suggesting again the formation of strong intermolecular hydrogen bonds.

It is interesting that temperature at which a film is assembled significantly influences the growth rate of the film. As shown in Figure 3, linear film growth was observed at all temperatures we studied; however, the film growth rate was different. Generally, as temperature increases, film growth rate decreases. For example, the growth rate at 30 °C is only ~60% of that at 10 °C. As a result, films fabricated at lower temperatures tend to

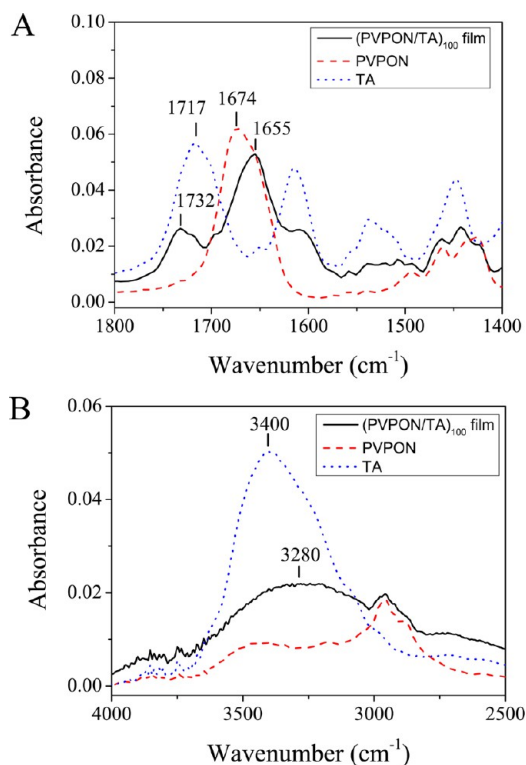


**Figure 2.** Carbonyl stretching regime (A) and the hydroxyl stretching regime (B) of the FTIR spectra of PVPON, TA, and a (PVPON/TA)<sub>100</sub> film.

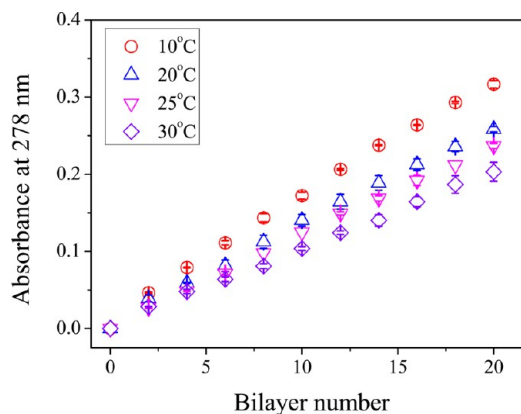


**Figure 3.** Growth of PVPON/TA films assembled at different temperatures as indicated in the figure.

be thicker. Assembly temperature also significantly influences the morphology of the resultant films. As shown in Figure 4, the film fabricated at 10 °C presents an extremely rough surface. Most of the film surface is occupied by irregular features with a size ranging from ~100 nm to several micrometers. With increasing assembly temperature, however, both the number and the size of these features decrease significantly; therefore, the film surface becomes much smoother. AFM images of the films also show that the film fabricated at a lower temperature is rougher (Figure S1 in Supporting Information). The calculated RMS (Root Mean Square) surface roughness is 19.2, 8.48, and 6.83 nm for the films fabricated at 10, 22, and 25 °C, respectively.

The temperature-dependent growth behavior of PVPON/TA films is very different from the traditional LbL films



**Figure 4.** SEM images of the (PVPON/TA)<sub>60</sub> films fabricated at 10 (A), 22 (B), and 25 °C (C), respectively.

fabricated using electrostatic interactions as driving forces. For the latter case, temperature usually does not have a strong, direct influence on the film growth, as it usually does not change the strength of electrostatic interactions between the charged groups.<sup>46</sup> In contrast, hydrogen bonding, which is used as the main driving force here, is highly susceptible to temperature change. It is well-known that the strength of hydrogen bonds decreases with increasing temperature.<sup>47</sup> For example, in the interpenetrated network hydrogels composed of polyacrylamide (PAAm) and polyacrylic acid (PAA), hydrogen bonds form between the two polymers at lower temperatures but dissociate at higher temperature, resulting in an UCST (upper critical solution temperature) behavior of the hydrogel.<sup>48–50</sup> Partial breakage of the hydrogen bonds in hydrogen-bonded LbL films upon heating was reported previously.<sup>21,51</sup> As for the present case, the hydrogen bonding between PVPON and TA is relatively strong at a low temperature, e.g., 10 °C. Therefore, when a PVPON-terminated surface is immersed in the TA solution, or vice versa, the PVPON/TA complex forms quickly at the interfaces, resulting in a rough surface. In addition, the strong interaction between PVPON and TA prevents the polymer chains from rearrangement and thus locks the morphology. However, at a relatively higher temperature, e.g., 25 °C, the hydrogen bonding between PVPON and TA is weakened; therefore, the PVPON/TA complex forms at a relatively slow rate. Chain arrangement in the film is also possible. As a result, the film surface is relatively smooth. Previously we<sup>30</sup> observed that rough LbL films were obtained from PVPON and PAA because of the strong hydrogen bonding between the two polymers. However, smooth films were obtained from PVPON–I (poly(vinyl pyrrolidone)–iodine complex) and PAA under the same conditions because the hydrogen bonding is weakened as a result of partial complexation of PVPON with iodine. The different film morphologies obtained at different temperatures further result in different film growth rates. At a low temperature, the rough film surface provides a larger effective surface area for the deposition of a next layer. Therefore, the film grows at a faster rate, as shown in Figure 3.

**Release of TA from the LbL Films.** As the main interaction between PVPON and TA in the LbL films is hydrogen bonding, which is reversible in nature, when soaked in aqueous solutions, the films disassemble gradually, thus releasing TA from the films to the media.

To study the effect of pH on TA release, the LbL films were soaked in phosphate buffers with various pHs, ranging from 5.0 to 8.5. As shown in Figure 5, TA release was observed in all these media. Previously,  $pK_a$  of TA in water was determined to be  $\sim 8.5$ .<sup>41</sup> For TA incorporated in the PVPON/TA films, an even higher  $pK_a$  is expected, considering that the phenolic

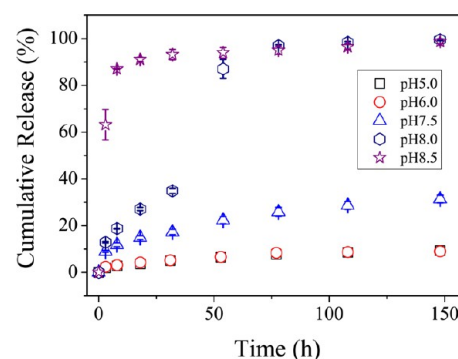


**Figure 5.** Release of TA from (PVPON/TA)<sub>60</sub> films in 20 mM phosphate buffers of various pHs.  $T = 37$  °C.

hydroxyl groups are strongly hydrogen-bonded with PVPON, as we showed above.<sup>52,53</sup> Therefore, at the pHs studied here, the dissociation degree of TA in the films should be low. In other words, the hydrogen bonds between TA and PVPON largely remain intact, especially at relatively lower pHs. The film disassembly under these conditions should be attributed to the shift of equilibrium of the following reaction because of the reversibility of the hydrogen bonding:



It has long been observed that various hydrogen-bonded films, for example, LbL films from PVPON and PAA, disintegrate quickly when soaked in aqueous solutions with high pHs.<sup>54</sup> In these cases, most of the carboxylic acid groups dissociate quickly, resulting in the breakage of the hydrogen bonds and thus a quick disintegration of the film. Particularly quick disintegration of PVPON/TA films has also been observed when the films are soaked in solutions with  $\text{pH} > 9$ ,<sup>41</sup> which is also achieved by the direct disruption of the hydrogen bonds as a result of the dissociation of the phenolic hydroxyl groups at high pHs. In these cases, one can only achieve a burst release of the film materials.

In contrast, the film disassembly via the shift of the equilibrium of the reversible formation and breakage of hydrogen bonds, as we show here, results in a slow and sustained release of TA. In addition, the release process can be finely controlled by external conditions. From Figure 5, one can see that TA release becomes faster with increasing pH. At low pHs such as 5.0 and 6.0, TA release is very slow. After a 148 h immersion, only  $\sim 9\%$  of TA is released. In contrast, in pH 8.5 buffer, about 90% of TA is released within 8 h. Long-term release profiles of TA at pHs 5.0, 6.0, and 7.5 were shown in Figure S2 (Supporting Information). At pH 7.5, all TA is released into the media in 1 month. At pH 5.0 and 6.0, only

41% and 54% of TA is released during a 2-month immersion. The faster TA release at higher pHs should be attributed to the increased dissociation degree of TA. Partial dissociation of the phenolic hydroxyl groups weakens the hydrogen bonding between TA and PVPON and hence increases the rate of film disassembly. In addition, the electrostatic repulsion among the charged TA molecules also accelerates the film disassembly. The increased solubility of TA molecules after dissociation may also contribute to the faster TA release.

To study the effect of ionic strength, PVPON/TA films were soaked in 20 mM pH 7.5 phosphate buffers containing various amounts of NaCl. The release profiles were shown in Figure 6.

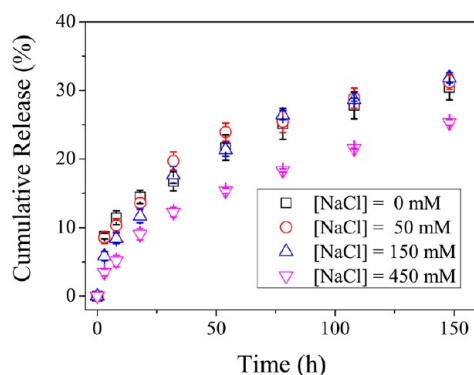


**Figure 6.** Release of TA from (PVPON/TA)<sub>60</sub> films in 20 mM pH 7.5 phosphate buffers containing various concentrations of NaCl.  $T = 37\text{ }^{\circ}\text{C}$ .

One can see that compared with the release rate in the NaCl-free media the change in the release rate is negligible when [NaCl] is 50 or 150 mM. As shown in Figure 5, the release rate of TA at pH 7.5 is larger than that at pHs 5.0 and 6.0, indicating a small amount of TA is dissociated at this pH. The added NaCl may screen the electrostatic repulsions among the charged TA molecules, resulting in a reduced TA release. In addition, the solubility of both TA and PVPON should decrease with increasing ionic strength, which will also delay the release of TA. However, the added NaCl may also enhance the dissociation of the phenolic hydroxyl groups in TA, leading to the breakage of more hydrogen bonds and therefore a faster TA release. The combined result is that the added NaCl does not change the release rate of TA at these NaCl concentrations. However, further increasing [NaCl] to 450 mM results in a significantly depressed TA release, suggesting the prevailing effect of salt in this case is to delay the release of TA.

The effect of temperature on the release of TA was shown in Figure 7. Here the LbL films were immersed in 20 mM pH 7.5 phosphate buffer at various temperatures. One can see that the release rate of TA increases dramatically as temperature increases from 25 to 45 °C. At 25 °C, only ~10% of TA is released after 150 h immersion. The amount increases to 31% at 37 °C and even ~100% at 45 °C. The accelerated release of TA should be attributed to the increased dissociation of the hydrogen bonds at high temperature. As mentioned above, heat-induced partial breakage of the hydrogen bonds in the hydrogen-bonded LbL films, for example, the LbL films from PVPON and *m*-methylphenol-formaldehyde resin or PAA, has been confirmed by IR spectra.<sup>21,51</sup> Similarly, the hydrogen bonding between PVPON and TA should also weaken as temperature increases; therefore, the films disassemble and release TA at a faster rate.

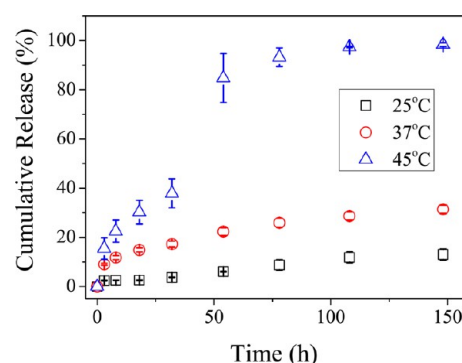


**Figure 7.** Release of TA from (PVPON/TA)<sub>60</sub> films in 20 mM pH 7.5 phosphate buffer at various temperatures.

**Changes in Film Morphology.** The morphology changes of the film during TA release were studied. At predetermined intervals, the films were withdrawn from the release media and examined with SEM and AFM. A general trend is that the amount of the particle-like features reduces gradually, and the film surface becomes smoother. This observation may partially explain the gradual decrease of the release rate of TA. As the film surface becomes smoother, the effective surface area decreases accordingly; therefore, the release rate of TA decreases.

Special attention was paid to the sudden increased release rate in certain cases, i.e., the releases in pH 8.0 buffer at 37 °C as shown in Figure 5 and in pH 7.5 buffer at 45 °C as shown in Figure 7. These experiments were repeated several times, and the sudden accelerated release was observed at almost the same release time. Figure 8 shows the morphology of a film immersed in pH 8.0 buffer at 37 °C as observed by SEM. One can see that the film first becomes smoother with time and even featureless after 32 h immersion. Similar results were obtained when studied by AFM (Figure S3 in Supporting Information). The calculated RMS roughness of the film decreases from 8.32 nm to only 0.42 nm after a 32 h immersion. A possible explanation is that the erosion rate is faster for the protruded features because of their larger effective surface areas, and therefore these features become less prominent and finally almost disappear. From then on, the film becomes rougher again when examined after a 40 h immersion. We believe the increased roughness is a result of the dewetting of the film. It is well-known that thin polymer films are unstable or metastable. Under proper conditions, dewetting or the relaxation of the system towards thermodynamical equilibrium can occur, especially when the film is thinner than a critical thickness.<sup>55,56</sup> Film dewetting usually results in small holes, which were clearly observed from the film with an even longer immersion (Figure 8I). Most holes are round in shape with a size of ~100 nm. It is noteworthy that the dewetting of some LbL films has previously been reported.<sup>31,57–61</sup> From the results shown in Figures 5 and 8, the onset of the film dewetting and the sudden accelerated TA release occurs at almost the same time. These observations suggest that with the gradual erosion of the film the film thickness reduces to a critical value, and the dewetting of the film starts. Film dewetting results in a rougher surface, providing a much larger effective surface area, and therefore the TA release rate increases sharply.

**Antioxidant Activity of the Released TA.** A major biological activity of polyphenols, including TA, is their antioxidant activity, which is believed to be the main reason

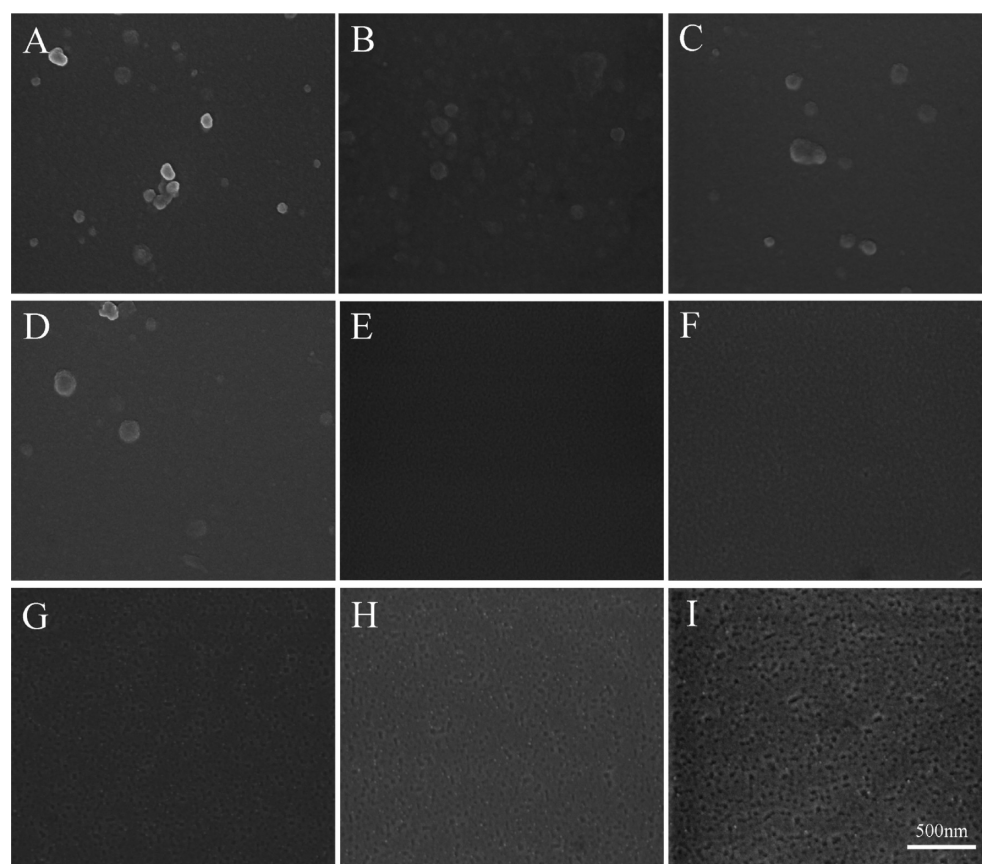


**Figure 8.** SEM images of a  $(\text{PVPON/TA})_{60}$  film after being soaked in 20 mM pH 8.0 phosphate buffer for 0, 3, 8, 18, 32, 40, 48, 54, and 80 h.  $T = 37$  °C.

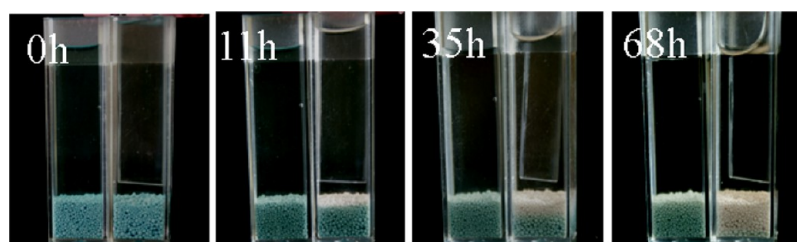


**Figure 9.** Decolorization of  $\text{ABTS}^{\bullet+}$ -loaded macroporous adsorption resin in the presence (right) or absence (left) of  $(\text{PVPON/TA})_{150}$  film. The media is 20 mM pH 8.5 phosphate buffer.  $T = 27$  °C.

for the protective effects of polyphenols.<sup>62</sup> Some cancers are related to oxygen-centered free radicals and other reactive oxygen species, which, if overproduced, cause oxidative damage to DNA, proteins, and other important biomolecules. Polyphenols can scavenge these species effectively and thus provide protection to the body. Previously, the radical cation  $\text{ABTS}^{\bullet+}$  was used for the determination of the antioxidant activity of various materials.<sup>44</sup> This radical cation is stable and blue/green in color. It can be easily generated by the oxidation of ABTS with potassium persulfate. Reaction of an antioxidant with the radical cation results in the decolorization of the solution, from which the antioxidant activity can be determined. Here we also used this method to show the antioxidant activity of TA released from the LbL film.

For this purpose, the  $\text{ABTS}^{\bullet+}$  radical cation was first generated using the literature method.<sup>44</sup> The UV–vis spectra of the resultant solution present characteristic peaks of the radical cation at 415, 645, 734, and 815 nm, respectively (data

not shown). The radical cation was then immobilized onto macroporous adsorption resin. With the adsorption of the  $\text{ABTS}^{\bullet+}$  radical cation, the originally white resin particles turned blue. The resin particles were then soaked in phosphate buffer together with a PVPON/TA film. pH 8.5 buffer was used because TA release is relatively fast at this pH. As shown in Figure 9, the particles were decolorized gradually from top to bottom. As a control, the color change of the  $\text{ABTS}^{\bullet+}$ -loaded resin particles in the absence of PVPON/TA film was also studied. In this case, only a slight change in color was observed. These results indicate that the released TA can still react with the  $\text{ABTS}^{\bullet+}$  radical cation and decolorize it, suggesting it remains active as an antioxidant to scavenge free radicals.

## CONCLUSIONS

In conclusion, we achieved the sustained release of TA, a model polyphenolic drug, from hydrogen-bonded PVPON/TA films. Different from the mechanisms used before, we exploited the

reversible/dynamic nature of the hydrogen-bonded films for sustained drug delivery. TA is released to the media as a result of the gradual disassembly of the film in aqueous solutions. The released TA retains its ability to scavenge harmful radicals, which can cause cancer and other diseases. Besides polyphenolic drugs, other drugs, if conjugated with a polyphenolic compound, can also be released using the newly developed strategy.

As a new drug delivery vehicle, hydrogen-bonded LbL film provides a lot of advantages. The drug-loaded films can be coated to various medical devices with different shape and size. The amount of drug loaded in the film can be facilely controlled by the bilayer number of the films. In addition, the drug release rate can be tuned by both temperature and pH because hydrogen bonding is highly sensitive to these external stimuli.

## ■ ASSOCIATED CONTENT

### ● Supporting Information

AFM images of the film and long-term release profile of TA. This material is available free of charge via the Internet at <http://pubs.acs.org>.

## ■ AUTHOR INFORMATION

### Corresponding Author

\*Tel.: +86-22-23501657. Fax: +86-22-23503510. E-mail: [yongjunzhang@nankai.edu.cn](mailto:yongjunzhang@nankai.edu.cn).

### Notes

The authors declare no competing financial interest.

## ■ ACKNOWLEDGMENTS

We thank financial support for this work from the National Natural Science Foundation of China (Grants Nos. 21174070, 21274068, and 21228401), Tianjin Committee of Science and Technology (10JCYBJC02000), Program for New Century Excellent Talents in University (NCET-11-0264), and the Ministry of Science and Technology of China (Grant No.: 2007DFA50760).

## ■ REFERENCES

- (1) Decher, G. *Science* **1997**, *277*, 1232–1237.
- (2) Ariga, K.; Ji, Q.; Hill, J. P.; Bando, Y.; Aono, M. *NPG Asia Mater.* **2012**, *4*, e17.
- (3) Matharu, Z.; Bhandekar, A. J.; Gupta, V.; Malhotra, B. D. *Chem. Soc. Rev.* **2012**, *41*, 1363–1402.
- (4) Tang, Z. Y.; Wang, Y.; Podsiadlo, P.; Kotov, N. A. *Adv. Mater.* **2006**, *18*, 3203–3224.
- (5) Wohl, B. M.; Engbersen, J. F. J. *J. Controlled Release* **2012**, *158*, 2–14.
- (6) Zelikin, A. N. *ACS Nano* **2010**, *4*, 2494–2509.
- (7) Tong, W. J.; Gao, C. Y. *J. Mater. Chem.* **2008**, *18*, 3799–3812.
- (8) Antipov, A. A.; Sukhorukov, G. B. *Adv. Colloid Interface Sci.* **2004**, *111*, 49–61.
- (9) Ye, S.; Wang, C.; Liu, X.; Tong, Z.; Ren, B.; Zeng, F. *J. Controlled Release* **2006**, *112*, 79–87.
- (10) Ibarz, G.; Dahne, L.; Donath, E.; Mohwald, H. *Adv. Mater.* **2001**, *13*, 1324–1327.
- (11) Peyratout, C. S.; Dahne, L. *Angew. Chem., Int. Ed.* **2004**, *43*, 3762–3783.
- (12) Dai, Z. F.; Heilig, A.; Zastrow, H.; Donath, E.; Mohwald, H. *Chem.–Eur. J.* **2004**, *10*, 6369–6374.
- (13) Chen, X.; Wu, W.; Guo, Z.; Xin, J.; Li, J. *Biomaterials* **2011**, *32*, 1759–1766.

- (14) Ding, Z. B.; Guan, Y.; Zhang, Y. J.; Zhu, X. X. *Polymer* **2009**, *50*, 4205–4211.
- (15) Flessner, R. M.; Jewell, C. M.; Anderson, D. G.; Lynn, D. M. *Langmuir* **2011**, *27*, 7868–7876.
- (16) Blacklock, J.; Handa, H.; Manickam, D. S.; Mao, G.; Mukhopadhyay, A.; Oupicky, D. *Biomaterials* **2007**, *28*, 117–24.
- (17) Smith, R. C.; Riollano, M.; Leung, A.; Hammond, P. T. *Angew. Chem., Int. Ed.* **2009**, *48*, 8974–8977.
- (18) Wojtecki, R. J.; Meador, M. A.; Rowan, S. J. *Nat. Mater.* **2011**, *10*, 14–27.
- (19) Lehn, J. *Prog. Polym. Sci.* **2005**, *30*, 814–831.
- (20) Maeda, T.; Otsuka, H.; Takahara, A. *Prog. Polym. Sci.* **2009**, *34*, 581–604.
- (21) Zhang, Y. J.; Guan, Y.; Yang, S. G.; Xu, J.; Han, C. C. *Adv. Mater.* **2003**, *15*, 832–835.
- (22) Lee, H.; Mensire, R.; Cohen, R. E.; Rubner, M. F. *Macromolecules* **2011**, *45*, 347–355.
- (23) Stockton, W. B.; Rubner, M. F. *Macromolecules* **1997**, *30*, 2717–2725.
- (24) Wang, L.; Wang, Z.; Zhang, X.; Shen, J.; Chi, L.; Fuchs, H. *Macromol. Rapid Commun.* **1997**, *18*, 509–514.
- (25) Suntvich, R.; Shchepelina, O.; Choi, I.; Tsukruk, V. V. *ACS Appl. Mater. Interfaces* **2012**, *4*, 3102–3110.
- (26) Ma, L.; Cheng, M.; Jia, G.; Wang, Y.; An, Q.; Zeng, X.; Shen, Z.; Zhang, Y.; Shi, F. *Langmuir* **2012**, *28*, 9849–9856.
- (27) Zhang, Y. J.; Cao, W. X. *Langmuir* **2001**, *17*, 5021–5024.
- (28) Shimazaki, Y.; Mitsuishi, M.; Ito, S.; Yamamoto, M. *Langmuir* **1997**, *13*, 1385–1387.
- (29) Zhang, X.; Chen, H.; Zhang, H. Y. *Chem. Commun.* **2007**, 1395–1405.
- (30) Guan, Y.; Yang, S. G.; Zhang, Y. J.; Xu, J.; Han, C. C.; Kotov, N. A. *J. Phys. Chem. B* **2006**, *110*, 13484–13490.
- (31) Lin, W.; Guan, Y.; Zhang, Y. J.; Xu, J.; Zhu, X. X. *Soft Matter* **2009**, *5*, 860–867.
- (32) Guan, Y.; Zhang, Y. J.; Zhou, T.; Zhou, S. Q. *Soft Matter* **2009**, *5*, 842–849.
- (33) Ding, Z. B.; Guan, Y.; Zhang, Y.; Zhu, X. X. *Soft Matter* **2009**, *5*, 2302–2309.
- (34) Daglia, M. *Curr. Opin. Biotechnol.* **2012**, *23*, 174–181.
- (35) Akagawa, M.; Suyama, K. *Eur. J. Biochem.* **2001**, *268*, 1953–1963.
- (36) Yang, C. S.; Ju, J.; Lu, G.; Xiao, H.; Hao, X.; Sang, S.; Lambert, J. D. *Asia-Pac. J. Clin. Nutr.* **2008**, *17* (S1), 245–248.
- (37) Shutava, T. G.; Balkundi, S. S.; Vangala, P.; Steffan, J. J.; Bigelow, R. L.; Cardelli, J. A.; O'Neal, D. P.; Lvov, Y. M. *ACS Nano* **2009**, *3*, 1877–1885.
- (38) Hsieh, D.; Lu, H.; Chen, C.; Wu, C.; Yeh, M. *Int. J. Nanomed.* **2012**, *7*, 1623–1633.
- (39) Costa, E.; Coelho, M.; Ilharco, L. M.; Aguiar-Ricardo, A.; Hammond, P. T. *Macromolecules* **2011**, *44*, 612–621.
- (40) Shutava, T.; Prouty, M.; Kommireddy, D.; Lvov, Y. *Macromolecules* **2005**, *38*, 2850–2858.
- (41) Erel-Unal, I.; Sukhishvili, S. A. *Macromolecules* **2008**, *41*, 3962–3970.
- (42) Lisunova, M. O.; Drachuk, I.; Shchepelina, O. A.; Anderson, K. D.; Tsukruk, V. V. *Langmuir* **2011**, *27*, 11157–11165.
- (43) Kozlovskaya, V.; Harbaugh, S.; Drachuk, I.; Shchepelina, O.; Kelley-Loughnane, N.; Stone, M.; Tsukruk, V. V. *Soft Matter* **2011**, *7*, 2364–2372.
- (44) Re, R.; Pellegrini, N.; Proteggente, A.; Pannala, A.; Yang, M.; Rice-Evans, C. *Free Radical Biol. Med.* **1999**, *26*, 1231–1237.
- (45) Shutava, T. G.; Balkundi, S. S.; Lvov, Y. M. *J. Colloid Interface Sci.* **2009**, *330*, 276–283.
- (46) Bertrand, P.; Jonas, A.; Laschewsky, A.; Legras, R. *Macromol. Rapid Commun.* **2000**, *21*, 319–348.
- (47) Dougherty, R. C. *J. Chem. Phys.* **1998**, *109*, 7372–7378.
- (48) Aoki, T.; Kawashima, M.; Katono, H.; Sanui, K.; Ogata, N.; Okano, T.; Sakurai, Y. *Macromolecules* **1994**, *27*, 947–952.

- (49) Xiao, X. C.; Chu, L. Y.; Chen, W. M.; Wang, S.; Li, Y. *Adv. Funct. Mater.* **2003**, *13*, 847–852.
- (50) Echeverria, C.; Lopez, D.; Mijangos, C. *Macromolecules* **2009**, *42*, 9118–9123.
- (51) Yang, S. G.; Zhang, Y. J.; Yuan, G. C.; Zhang, X. L.; Xu, J. A. *Macromolecules* **2004**, *37*, 10059–10062.
- (52) Burke, S. E.; Barrett, C. J. *Langmuir* **2003**, *19*, 3297–3303.
- (53) Choi, J.; Rubner, M. F. *Macromolecules* **2005**, *38*, 116–124.
- (54) Sukhishvili, S. A.; Granick, S. *Macromolecules* **2002**, *35*, 301–310.
- (55) Muller-Buschbaum, P. *J. Phys.: Condens. Matter* **2003**, *15*, R1549–R1582.
- (56) Xue, L.; Han, Y. *Prog. Polym. Sci.* **2011**, *36*, 269–293.
- (57) Qin, S.; Wei, D. S.; Liao, Q.; Jin, X. G. *Macromol. Rapid Commun.* **2006**, *27*, 11–14.
- (58) Fredin, N. J.; Zhang, J. T.; Lynn, D. M. *Langmuir* **2007**, *23*, 2273–2276.
- (59) Shim, B. S.; Podsiadlo, P.; Lilly, D. G.; Agarwal, A.; Leet, J.; Tang, Z.; Ho, S.; Ingle, P.; Paterson, D.; Lu, W.; Kotov, N. A. *Nano Lett.* **2007**, *7*, 3266–3273.
- (60) Zhang, J.; Fredin, N. J.; Lynn, D. M. *Langmuir* **2007**, *23*, 11603–11610.
- (61) Zhang, L.; Zheng, M.; Liu, X.; Sun, J. *Langmuir* **2011**, *27*, 1346–1352.
- (62) Huang, W.; Cai, Y.; Zhang, Y. *Nutr. Cancer* **2009**, *62*, 1–20.